Influence of resource definition on defining a WEC optimal size

Rémy CR Pascal, Félix Gorintin, Grégory S. Payne, David Darbinyan, and Yves Pérignon

Abstract—This work is a follow up from two previous studies which have been investigating the difference in wave resource between sites and the impact this has on the optimal Wave Energy Converter (WEC) size using scatter diagrams of the sites only. This study expands these works by using omni-directional spectra time series to describe the wave resource instead of scatter diagrams. Two well known wave energy test sites are considered: EMEC (Billia Crew) in the North of Scotland and the SEM-REV on the West coast of France. The sloped IPS buoy is used as a case study, and a succinct description is provided. As in previous work, only the hydrodynamic power capture is considered, and no power-take-off efficiency or cap are introduced. For both sites, around one full year of data is available. Using both the scatter diagrams and the spectra directly, WEC performance metrics are computed for each site and compared. The results show that using spectral time series instead of the scatter diagrams yield lower annual energy productions, and that the highest average capture width ratio is obtained for larger scale devices. Spectral time series allows also the establishment of a simple O&M model. The effect on device availability of annual planned downtime days, of annual failure rates of 1, 3 and 5 and of operability threshold of 2m and 2.5m are investigated. The results show that larger scales might indeed have higher availability, but are exposed to higher risks.

Index Terms—WEC optimization, scale, maintenance, resource definition

I. Introduction

THIS work is a follow up from two previous studies which have been investigating the difference in wave resource between sites and the impact this has on the optimal Wave Energy Converter (WEC) size using scatter diagrams of the sites only [1], [2]. This study expands these works by using omni-directional spectra time series to describe the wave resource instead of scatter diagrams. The principle is similar to the process employed in [3], but uses measured spectra instead of hindcast data which may increase the level of uncertainties [4], and explores the impact of such processes

over the WEC design period or scale.

Two well known wave energy test sites are considered: EMEC (Billia Crew) in the North of Scotland and the SEM-REV on the West coast of France. The same WEC is used, and a succinct description is provided. As in previous work, only the hydrodynamic power capture is considered, and no power-take-off (PTO) efficiency or cap are introduced.

For both sites, around one full year of data is available. This allows the estimation of the corresponding scatter diagram. Then, using both the obtained scatter diagrams and the spectra directly, the most relevant metrics introduced in [2] are computed for each site and compared. A discussion about the impact of using summary statistics (scatter diagram) of a site wave resource instead of a more complex description is investigated, and key points relative to the WEC optimal size are highlighted.

A second set of results introduces a finer analysis regarding the importance of the design period on WEC availability considerations. The time series of spectra allows the modeling of the device availability through the year. The impact of the WEC design period over the consequences of failure and of planned maintenance is investigated and discussed.

A. Abbreviations and acronyms

Acronyms	Definition
$hAEP$	hydrodynamic Annual Energy Production
C_{WR}	Capture Width Ratio
aC_{WR}	average Capture Width Ratio
WEC	Wave Energy Converter
PTO	Power take off
$LCoE$	Levelized Cost of Energy
O&M	Operation and Maintenance
T	Wave period
T_mCW	Mean capture width period
T_E	Energy period
H_S	Significant wave height
CW	Capture width
λ	WEC geometric scale

II. Site data

The following section describes the data sources for the two sites considered. For each site, a scatter diagram is computed based on the spectral time series. The scatter diagram resolution follows the recommendations of [5]: 1s for the energy period T_E, and 0.5m for the significant wave height H_S.

B. EMEC

The wave data at Billia Croo site was collected using a Datawell Mk3 Waverider buoy during the year 2017. The dataset covers almost a full year, with the exception of few short breaks, when the buoy was recovered for maintenance. The Waverider buoy was deployed at the southern part of the site in a location with nominal coordinates of 58°58.214′N 003°23.454′W. The spectrum for each 30-minute period was derived as the average of 9 spectra calculated from the raw displacement data, collected at 1.28Hz. The data was quality controlled on two levels. Raw displacement data was checked for missing data points and spikes, with a single QC flag assigned to each 30-minute series of displacement data. It was followed by QC of bulk wave parameters done for 1-month long time-series, with data being checked for rate of change and acceptable range. The Waverider buoys deployed at Billia Croo are calibrated and serviced on a regular basis.

C. SEM-REV

In situ data are gathered on the SEM-REV marine test site [6] - a 1 km2 restricted area located 12 nautical miles offshore of Le Croisic on the French Atlantic coast - as part of the whole infrastructure dedicated to the test at sea of marine renewable energy devices and components. Among other sensors, up to two Datawell Waverider Mk3 buoys have been moored on site since 2009 recording displacements nearly 1 km apart (East and West corners of the site), and one Waverider Mk3 buoy complements the measurement at a more offshore location nearly 30 nm west. The water depths for the locations inside SEM-REV perimeter reach 34 m and 36 m LAT respectively, with a tidal amplitude of up to 6.1 m. The currents on site remain below $0.5m.s^1$ for the vast majority of its environmental conditions and the tidal influence over significant wave height only begins to show for specific sea states during spring tides [7]. For the purpose of this study, buoy data recorded at the west mooring site over the year 2012 are solely used. Vertical displacements of the buoy recorded at 1.28 Hz are thus exploited over 1h time windows in order to compute omni-directional frequency spectra. Integral parameters are inferred from the spectral distribution of the energy density.

III. METHOD AND METRICS

D. WEC model

The WEC and its numerical model used for this study are described in details in [8], [9]. It is a floating WEC whose PTO system consists of an immersed tube, open at both ends with a piston sliding inside the tube. The immersed tube is rigidly connected to the float and energy is generated from the relative motion between the float - tube assembly and the piston. The water inside the tube provides the inertial reference to the PTO. A sketch of the device can be seen on the left of figure 1. For numerical modelling, the representation of the PTO has been simplified

and consists of a point mass connected to the float via a damper. The damper only allows translation between the point mass and the float along a specific inclined direction as can be seen on the right of figure 1. It should be noted that through this simplification, the hydrodynamics loads on the tube are neglected and the inertial reference against which the piston is reacting is considered as constant. This simplification was a trade-off to alleviate computational burden and render practical the parametric study and optimization work carried out on the concept (see [8]).
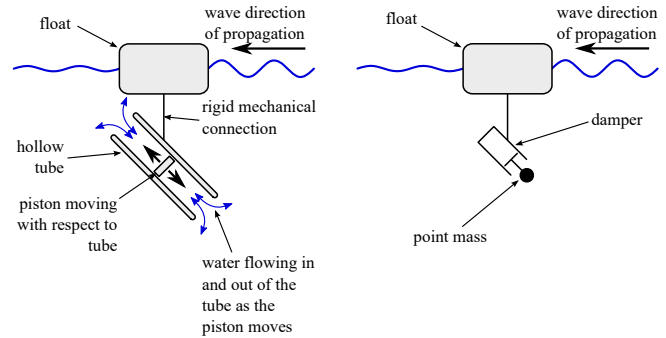

Fig. 1. Schematic of the WEC concept (left) and of its simplified representation for modelling purposes (right).

The float is a circular cylinder whose axis is vertical. At scale 1, the cylinder is 0.5m in diameter and draft and has a mass of 98kg. The optimization process on the PTO described in [8] led to a point mass of 98kg, located 0.25m below the centre of gravity of the float. The optimum damping value found is $326Nsm^{-1}$ associated with a damper angle of 50° to the vertical. The numerical modelling was carried out using WAMIT to compute the hydrodynamic coefficients on the float and the motions of the float and point-mass were then derived with a bespoke code as a two-body system.

E. WEC design period

Physically, the WEC design period loosely corresponds to the wave period around which the WEC has the best capture width performance. This is formally defined in [2] as corresponding to the mean capture width period, noted T_mCW and first introduced in [8]. When considering the capture width ratio curve of the WEC plotted against wave period, T_mCW is the mean of the wave period weighted by the capture width ratio over the period spectrum of interest:

$$T_mCW = \frac{1}{CW_{area}} \int_{spectrum} CW(T)TdT \qquad (1)$$

where CW_{area} is the area under the capture width curve, T the wave period and $CW(T)$ the WEC capture width value at period T.

The geometrical scale λ of the WEC with respect to scale 1 (as defined in section III-A) is related to the design period through Froude scaling as follows.

$$T_m CW_\lambda = \sqrt{\lambda} \cdot T_m CW_1 \qquad (2)$$

where $T_m CW_\lambda$ is the design period of the WEC at scale λ and $T_m CW_1$ is the design period of the WEC at scale 1.

The WEC C_{WR} curves obtained from the numerical model and upscaled (scales 11, 16, 23, 31, 41, 51) are presented in Fig. 2.
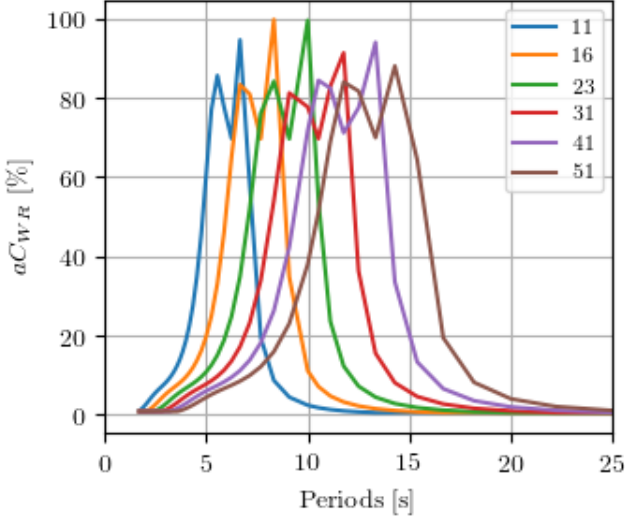

Fig. 2. WEC C_{WR} plotted against wave period for scales 11, 16, 23, 31, 41, 51. The curves are scaled up from the C_{WR} curve at scale 1 presented in [8], and interpolated to the period resolution of the Emec spectra.

F. WEC power from spectra

As in [2], the mean power produced by the WEC for a given omni-directional spectrum is obtained by multiplying in the frequency domain the spectrum and the WEC capture width ratio curve. The linear WEC power is then estimated in the same way as the incident power in a spectrum is computed.

It is however widely accepted that WEC hydrodynamic performances are decreasing as the sea state steepness is increasing. To avoid associating high energy, steep sea states with unrealisticly high WEC energy production, this performance drop should be modelled. In this work, a correction factor is therefore introduced, based on the steepness parameter S_s [10]. S_s values for the considered data varies from 0.01 to 0.08 approximately. For $S_s < 0.02$, the correction coefficient is set to 1. For values above, a cos^2 type function is used to provide a smooth decrease of the coefficient as S_S increases. The equation coefficients are selected such as $coef(S_S)|_{S_S=1} = 0$:

$$coef = \cos\left(\pi \frac{S_S - 0.02}{0.36}\right)^2 \qquad \text{for } S_S > 0.02 \quad (3)$$

Figure 3 shows the evolution of the correction coefficient as a function of S_S for the observed S_S range.
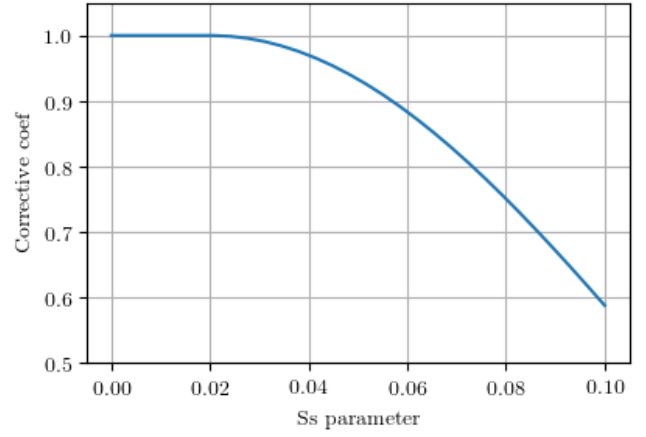

Fig. 3. WEC power corrective coefficient as a function of the sea state steepness S_s [10]. Max S_s in data is around 0.08.

For every spectra, the WEC power is estimated as $Power = coef(S_S) \cdot Power_{linear}$.

This correction coefficient is also applied to the power matrices which must be generated when estimating the metrics from the scatter diagrams. This is an evolution of the method used in [2], and therefore slightly different results could be observed.

G. Metrics

1) Metrics from previous study: The most relevant metrics from [2] are used again in this work. Those metrics are:

- the hydrodynamic annual energy produced ($hAEP$)
- the average capture width ratio (aC_{WR})
- percentage of $hAEP$ produced by discarding X% of the sea states, starting with lowest producing sea states.

Their complete definitions can be found in the previous study. They can be estimated either using the scatter diagrams of the sites, or directly the 1D spectra time series. These metrics can therefore be compared and the influence of the resource description on them can be discussed.

In addition to these metrics, further investigation is allowed by the use of 1D spectra time series. The method is described below.

2) Definition of availability metrics: In common $LCoE$ models, the device availability is a ratio used to take into account downtime on the annual power production of the device. Availability above 90% are normally expected for a commercially available device [11], however [12] mentioned that due difficulty of access to WECs, lower values might be expected.

[2] suggested that these ratio would potentially be affected by the device scale. In this study, the dependence of the device availability to the device scale is therefore investigated by simulating downtime through the year at both sites.

First, a planned downtime operation is considered, with possible duration of 20, 30 and 40 days. This

period is randomly located in the low production months, from May to July.

Second, a number of failures are simulated through the year. Failure rates of 1, 3 and 5 critical failures per year are considered. Failures are randomly allocated throughout the year. For each failure, the algorithm then identify the next available weather window for retrieving the device (12 hours with $H_S < 2m$). A 24-hour period is then added for the WEC repair. Finally, the next available weather window for device redeployment is identified (12 hours with $H_S < 2m$). From the failure to the end of the redeployment weather window, the device production is considered equal to 0. It should be noted that the algorithm ensures that a failure cannot occur during the downtime period triggered by a previous failure. The process involved could be more accurate, but was thought to be satisfactory for the purpose of the present study.

The procedure to simulate availability is iterated 2000 times for each failure rate and planned downtime duration considered. For each iterations, a device $hAEP$ is obtained for each scale. Their distributions and histograms can then be built and investigated.

IV. RESULTS

H. Comparing with scatter diagram

Fig. 4 and Fig. 5 present the evolution of the $hAEP$ and aC_{WR} for EMEC and SEM-REV sites respectively. Results from scatter diagram where obtained by generating JONSWAP spectra with γ of 1 and 3.3 from the H_S and T_E values. These results are compared with those of the model based on the actual spectra.

The first observation is that the expected $hAEP$ is lower if using the spectral time series, especially in the SEM-REV cases. In this latter case, as the aC_{WR} values are in the same order of magnitude, the difference in spectral shape between the actual spectra and the assumed JONSWAP is the main potential explanation for the large differences. The shallower depth at this site end extent of intermediate depth up wave associated to possible wave transformations, have notably been shown to significantly modify the spectral content near the peak for energetic sea states [4] [13]. Also, a slightly lower spectral resolution compared to EMEC data could have some influence on the computed quantities. The aC_{WR} plots also show clearly that using the actual spectra instead of a scatter diagram will induce the design of larger machine, with a higher design period. Indeed, in both cases, the peak of capture width ratio is moved towards the higher periods. There is some potential explanation for those observations, which could be explored in further details:

- the scatter diagram resolution is not high enough for the low energy, low periods sea states. This could lead to an overestimation of energy production;
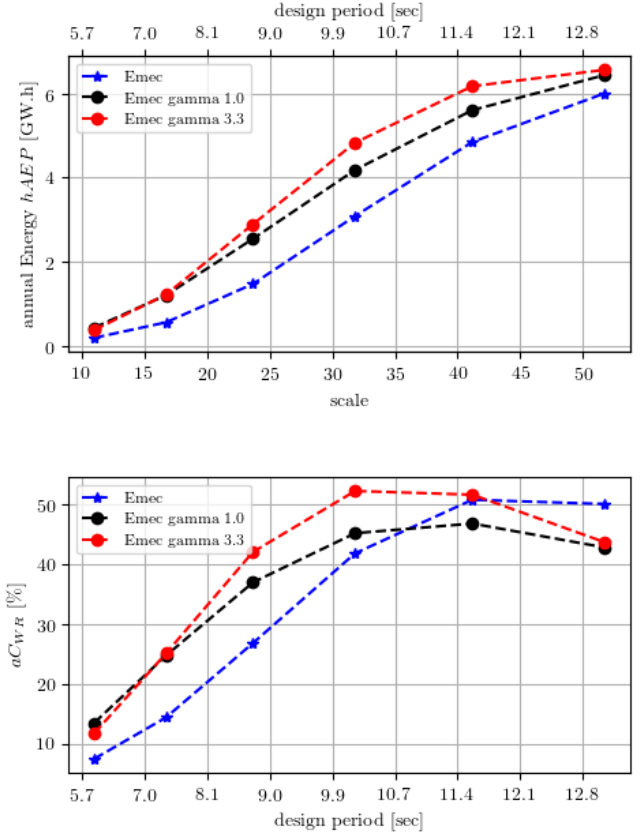

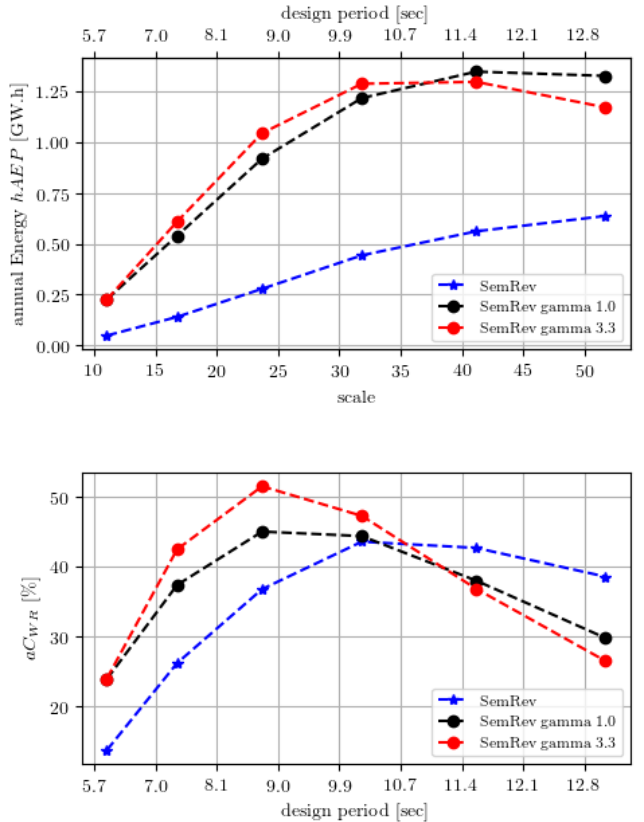Fig. 4. $hAEP$ and aC_{WR} for the EMEC site.

Fig. 5. $hAEP$ and aC_{WR} for the SEM-REV site.

- the spectral shapes for low periods, low energy sea states are very varied and are not well represented
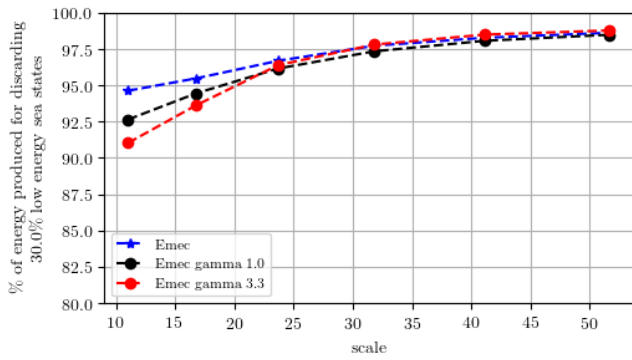
Fig. 6. Percentage of $hAEP$ at EMEC while discarding 30% of the sea states starting with the least energetic ones.
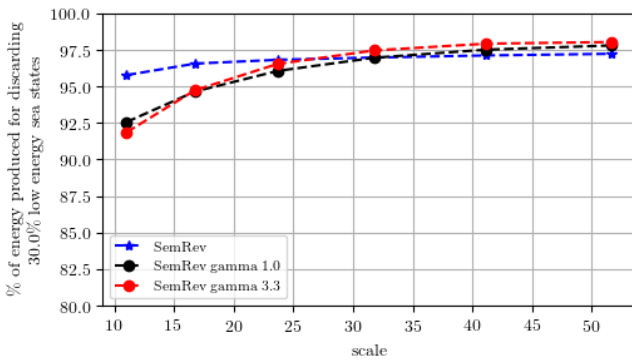

Fig. 7. Percentage of $hAEP$ at EMEC while discarding 30% of the sea states starting with the least energetic ones.

by a JONSWAP spectral shape.

Figure 6 and Fig. 7 show the effect of discarding the sea states with the lowest incident power representing 30% of the annual occurrences for each site. Results are shown as percentage of full $hAEP$ plotted against WEC scale. In both cases, the results shows that discarding the low energy sea states has a very limited impact on the annual WEC production. Using the spectral time series shows that the decrease in production is less dependant on scale than using the scatter diagrams. Overall, for both sites, and independently of scale, discarding up to 30% of the annual sea states (starting with the least energetic) does not decrease the $hAEP$ by more than 5%.

Fig. 8 to Fig. 11 show the histograms of the WEC mean powers associated with each sea state spectrum of the time series (discarding 30% of the sea states starting with the least energetic ones). The associated cumulative production in % is also shown. Results for scale 16 and 41 are presented, for both sites. In every cases, the histograms are concentrated to the left, towards the low power production sea states, with a long tail towards the high production sea states. The intersections between the mean, median, and 90 and 95 percentile with the normed cumulative production curve show that ignoring this long tail of high production sea states has a very large impact on the $hAEP$. Therefore, those histograms highlight the issue of dimensioning correctly a PTO for WECs:
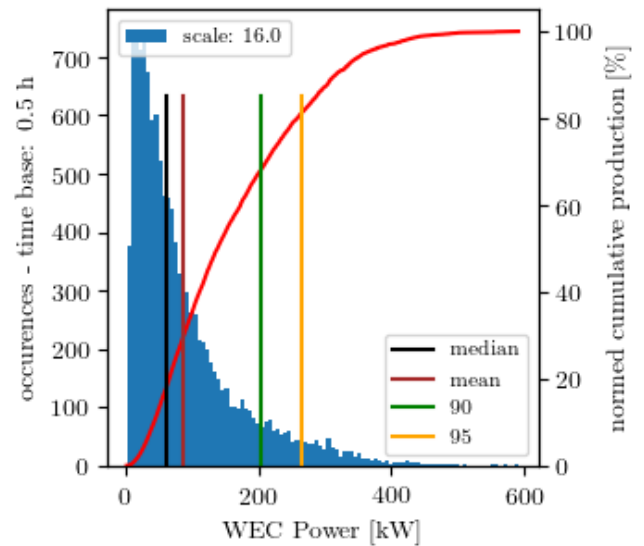

Fig. 8. Histogram and normed cumulative production of WEC mean powers, at EMEC for scale 16, after discarding 30% lowest incident power sea states. The median, mean, 90 and 95 percentiles are indicated.

dimension it for the mean or median production sea states, and it will probably no be able to absorb the large amount of power during the high energy sea states, and a large portion of the potential $hAEP$ will be lost. Dimension it for the high energy sea states, and the PTO will probably not be efficient for the low energy sea states. Finally, while contemplating this issue, it is important to remember that those power are only mean powers, and not instantaneous powers within a sea state, which will only increase the observed variability.

The plots however do show that scale has an effect: the device at scale 16 exhibits histograms that are less compressed to the left than the device at scale 41. This should therefore favour the development of smaller devices, for which the PTO rating problematics should be easier to solve. Similarly, the SEM-REV test site has smaller sea states, with smaller characteristics periods, and therefore at equal device scale, the histograms are more compressed at the SEM-REV sites.

I. Availability

[2] suggested that device scale for a given site should have strong impact on overall device availability. It also mentioned that the ratio of planned and unplanned maintenance should have different impacts depending on scale, with the largest devices being less impacted by planned maintenance.
Using the spectral time series, these claims can be examined and quantified. 2000 annual time series of WEC at each scale are generated as described in Section III-D2, for different annual failure rates (1, 3 and 5) and number of planned days of downtime (10, 20 , 30).

Figure 12 shows notched box-plot and whiskers plots representing the distribution of availabilities obtained
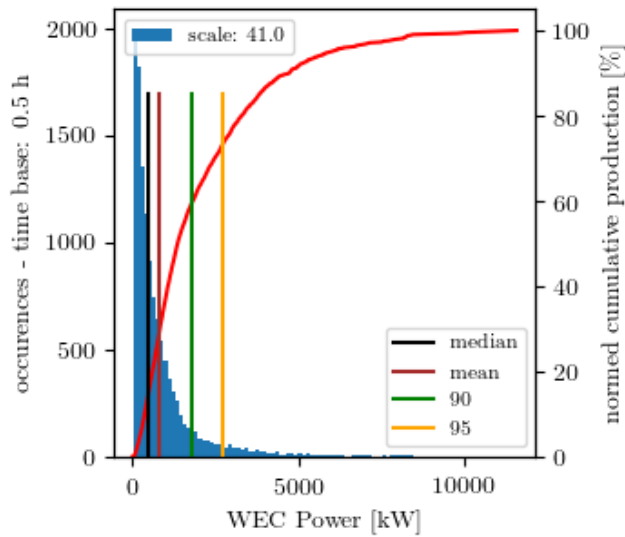
Fig. 9. Histogram and normed cumulative production of WEC mean powers, at EMEC for scale 41, after discarding 30% lowest incident power sea states. The median, mean, 90 and 95 percentiles are indicated.

Fig. 11. Histogram and normed cumulative production of WEC mean powers, at SEM-REV for scale 41, after discarding 30% lowest incident power sea states. The median, mean, 90 and 95 percentiles are indicated.
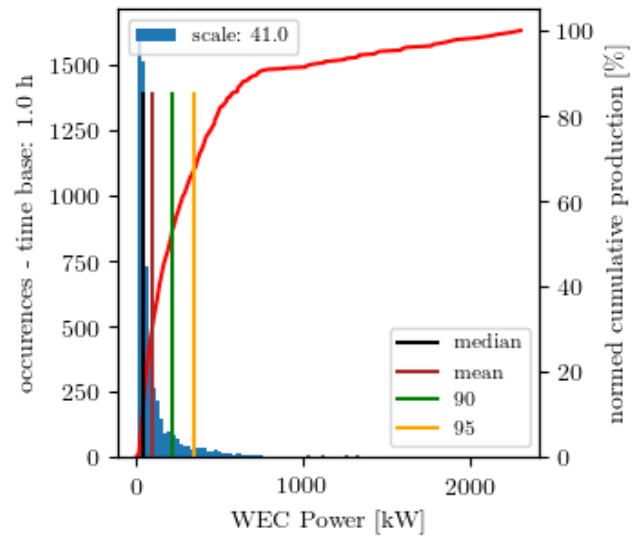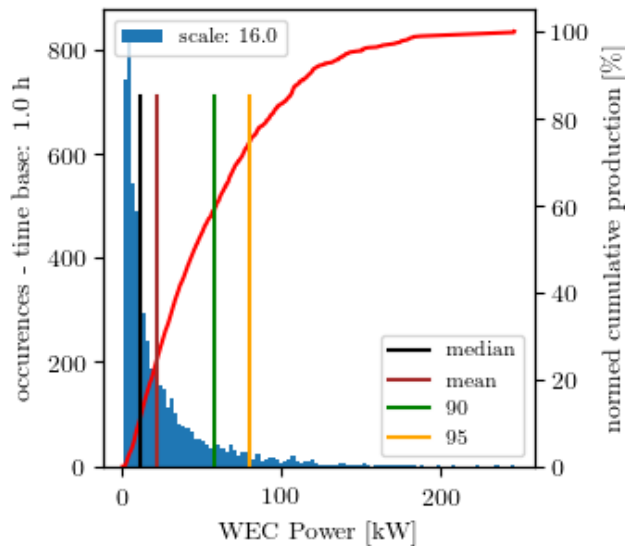

Fig. 10. Histogram and normed cumulative production of WEC mean powers, at SEM-REV for scale 16, after discarding 30% lowest incident power sea states. The median, mean, 90 and 95 percentiles are indicated.

at EMEC for each failure rate, days of planned downtime and scaled (figures at the SEM-REV site are not presented, the results are broadly similar).

First, the level of device availability are consistent with the hypothesis commonly used ($\sim$ 90%) in $LCoE$ models. A failure rate lower than or equal to 3 per year is required, and for any scale, bringing the failure rate down to 1 per year can raise the availability to 95%. Of course the O&M model used is simple, and more accurate numbers would be obtained from a model specific to a particular WEC.

One can clearly observe from these simulations that increasing the planned maintenance is more

detrimental to small devices, whereas increasing the failure rate has a strong effect on all scales. Indeed, along each column, increasing the number of planned days of downtime only appears to decrease the availabilities of the small devices. The effect however is limited compared to the effect of increasing the failure rate. Along each lines (same number of planned downtime, but increasing failure rate), the availability of the smaller devices is lower for the most reliable device (failure rate of one a year), but as the failure rate increases, the availability of the larger devices is decreasing at a higher rate. For the case of 10 days of downtime (top row), the availability of larger devices is indeed lower than the one of small devices for the high failure rate case.

Finally, the most important observations is probably that an O&M model that estimates median availability > 90% is also predicting availability in some cases as low as 60%. The model is also showing that in all cases, the spread between the 1% percentile and the median (or mean) is increasing for larger devices, confirming the expectation from [2] that for the same concept, going to larger scales increase the risk to the annual production of the device.

More details on the distribution of $hAEP$ can be obtained by examining histograms of the 2000 availabilities for the different scales and failures rates. Figure 13 shows the availability histograms at EMEC for each scale, assuming 10 days of planned downtime, and a failure rate of 3 per year. The histograms show that indeed the majority of the simulation yielded mean availability close to 90% for all the scales. However, the risk to have a year with actually very low availability is shown to be higher for the large scale devices: occurrences as low as 60% availability are observed for the largest scale. Interestingly, the
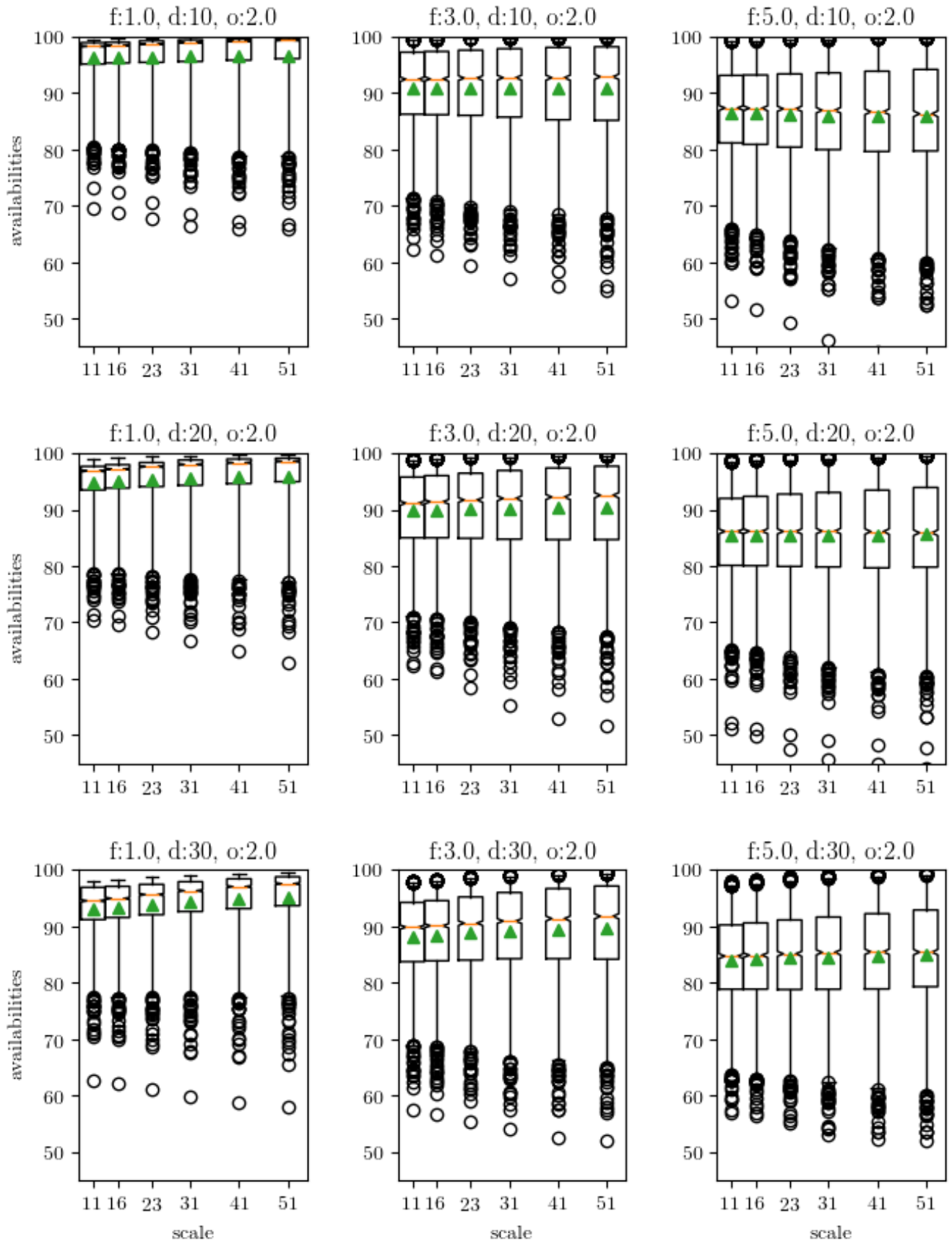
Fig. 12. Notched boxplots of availability's for each failure rate and planned downtime days at EMEC as a function of the device scale. The green triangles represents the means, the orange lines the median. The whiskers are set a the 1% an 99% percentile. Black circle represents outliers. Title represent f for failure rate, d for planned downtime days, o for operability (H_S in m).
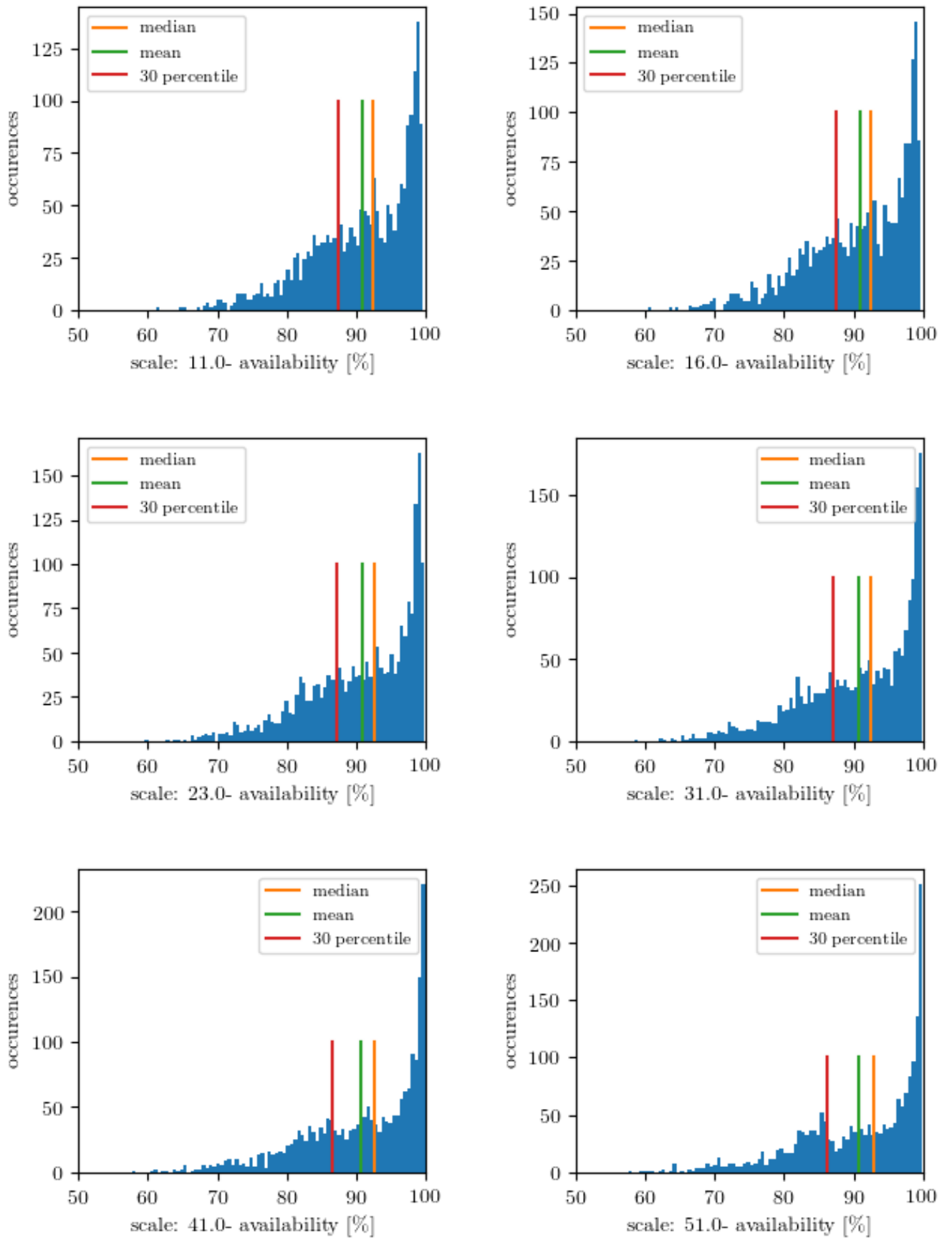
Fig. 13. Histograms of availabilities at EMEC, assuming a failure rate =3, 10 days of annual planned downtime, and an operability limit of $H_S = 2.0m$.
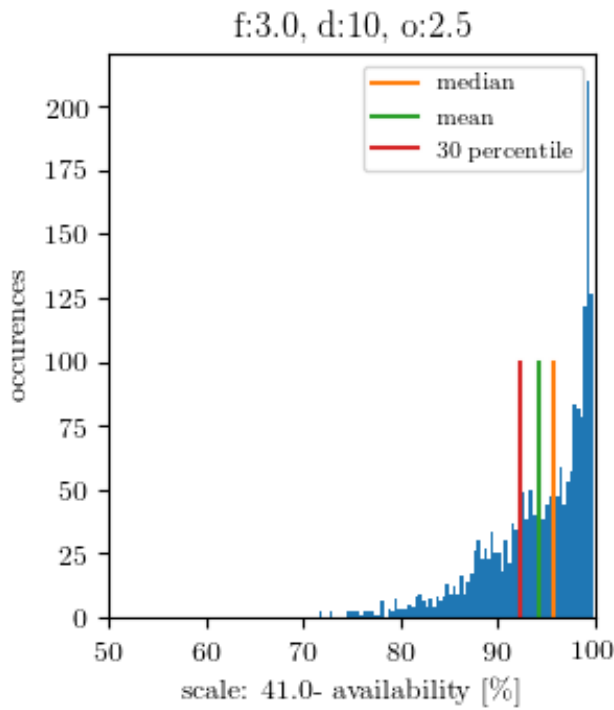
Fig. 14. Histogram of availabilities at EMEC, for scale 41 and assuming a failure rate =3, and 10 days of annual planned downtime, and an operability at $H_S = 2.5$

histograms show that for all cases, the distribution is very far from a normal distribution. Approximating these distributions with parametric functions would be useful as inputs for LCoE modelling, with the ability to realistically take into account the variability of the $hAEP$ due to device availability (this is different from variation from year on year resource variability). This possibility arises directly from the availability of spectral time series, and could not be obtained from the scatter diagram alone.

Fig. 14, represents the availability distribution of the device at scale 41, for the case failure rate=3 and 10 days of planned down time, but raising the operability limit to $H_S = 2.5m$. The figure should be compared to the subplot corresponding to the same scale (bottom left) of Fig. 13. Raising the operability has clearly lifted the mean and median availability a few percent up towards 95%, but maybe more significantly, the histogram is more compressed to the right, with only one occurrence below 74%, whereas there is multiple ones close to 60% in the Fig. 13 subplot. The risk to the device availability is clearly reduced.

V. DISCUSSION

First and foremost, it is important to keep in mind that the results presented in this article are linked to the particular WEC considered, and the hypotheses made to estimate its hydrodynamic performances and its O&M strategy. A different WEC, with different performances and variation in the method employed could potentially produce very different results. It would indeed be valuable to investigate in details

the validity of the hypotheses made and their effect on the results. Nonetheless, the study presented here highlights the benefits of using a detailed resource description and some of the challenges of WEC design. WEC developers are generally encouraged to adapt the method to their specific case and reproduce some of the results presented.

The use of spectral time series instead of scatter diagram first appears to have an important effect on the actual optimal size of a WEC from a point of view of maximising the potential for hydrodynamic energy capture. In both cases, the curve of capture width ratio obtained using the spectral time series peaks at a higher design period or scale than the ones drawn from the scatter diagrams. Additionally, the use of scatter diagrams with theoretical spectra is clearly leading to an overestimation of the device $hAEP$ at all scales investigated. The two sites exhibit different results: the $hAEP$ estimations at SEM-REV exhibit much larger differences between the methods. The first and obvious possible reason to explain these observations are the differences between the theoretical spectra considered when building the required power matrix and the actual real spectra ([3], [14]). As a matter of fact, the large departure of spectral measurements compared to modeled distributions in the most energetic sea states has already been documented on SEM-REV, which lead to significant reduction of the available energy around the theoretical spectral peak [4] [13]. The large extent of intermediate to shallow depths on the path of propagation for the incoming sea states remains at this stage a good candidate for spectral transformation and misfit of standard distributions. A second possible explanation is related to the resolution of the scatter diagrams and related power matrices. The typical resolution is 1s in T_E and 0.5m in H_S. At the short periods, H_S is limited and therefore a band of 0.5m might induces a significant relative error, which could possibly introduce a positive bias towards small scale devices which are more efficient at such periods. On the contrary, larger periods are most normally associated to higher H_S, and therefore errors of $\pm 0.25m$ are comparatively less significant. As the SEM-REV site is, on average, less energetic than EMEC, it should be comparatively more impacted by this issue. This could therefore be part of the reason why the differences in $hAEP$ estimation at SEM-REV are more important than at EMEC.

Further study on this specific issue could provide guidance about an adequate resolution of scatter diagrams and associated power matrices, especially for low to medium resource sites. In any cases, the observed differences should encourage WEC designers and evaluators to seek the use of spectral time series early in the design process and in the evaluation of the concepts. Using spectral time series, or at least time series of sea states parameters, at an early stage of design also highlights the difficulties regarding PTO dimensionning. Deciding on a PTO rating is indeed always a compromise. The distributions of

mean powers through the year, even after discarding the less energetic sea states representing up to 30% of the annual occurrences, show that the compromise might indeed be difficult to satisfy successfully without including complex features in the PTO such as intermediate storage and multiple generators. The study also shows that for a given concept, a choice of a smaller scale device will reduce the difficulty, suggesting again that early stage development of a concept should favour comparatively smaller scale devices, with maybe less complex PTO (without intermediate storage, or with a single generator).

The use of spectral time series allowed also the confirmation of the hypothesis presented at the end of [2], i.e. that larger device might have a higher availability than smaller devices for a given level of reliability, but these higher availabilities are associated with a higher risk. The larger devices would also be installed in smaller number for a given farm's installed power, and therefore the risk associated to the production of a single devices would potentially be more important. Additionally to the observed risk to the production, it should be noted that the failure model considered is not linked to sea states or device condition. It is however reasonable to assume that the risk of failure should be higher in energetic sea states, and it is therefore possible that a failure model taking this into consideration would yield even higher risk to the device $hAEP$. These high risks are linked to the dependency of $hAEP$ to the rarely occurring but most energetic sea states. A model capping its production for high H_S, or a concept drastically reducing its C_{WR} for higher sea states will exhibits lower risks to its $hAEP$. This benefit is additional to the higher survivability often put frontward for such concept, but seldom emphasized. The observed differences of availabilities between the device scale are not very large (around 4% of mean and median availability variation at most), and are smaller than what could be anticipated. Taking them into account might nonetheless have an effect on the selection of a device size based on $LCoE$ models (see [15]). Further study could focus, for a given case, on the characterisation of the availabilities distribution as a function of the device scale, and on the effect of employing such distribution to model uncertainty in an $LCoE$ model following a Monte-Carlo approach.

Finally, this approach allows to evaluate at an early stage in the design process the influence of the operability limits on the concept power production. While the operability strategy used for the simulation in this study is not entirely realistic, and not based on actual characteristics of the device, it provides insight into the very high impact that the operability has on the actual device power production, and on the reduction of the risk associated .

Contribution

Rémy CR Pascal conducted the main part of the study, and drafted most of the article. Grégory S. Payne developed the WEC hydrodynamic numerical model, wrote its description and reviewed the manuscript. , David Darbinyan and Yves Pérignon provided and described the sea state data for EMEC and SEM-REV respectively. Félix Gorintin advised on the development of the O&M strategy and reviewed the manuscript.

References

[1] R. C. R. Pascal, A. Torres Molina, and A. Gonzalez Andreu, "Going further than the scatter diagram : tools for analysing the wave resource and classifying sites," in *Proceedings of the 11th European Wave and Tidal Energy Conference*, Nantes, France, 2015, pp. 5–12.

[2] R. C. R. Pascal, F. Gorintin, G. S. Payne, and V. Cliquet, "The right size for a WEC : a study on the consequences of the most basic design choice ." in *Proceedings of the 7th International Conference on Ocean Energy*, Cherbourg, France, 2018.

[3] C. Maisondieu and M. Le Boulluec, "Benefits of using a spectral hindcast database for wave power extraction assessment," *The International Journal of Ocean and Climate Systems*, vol. 7, no. 3, pp. 83–87, 2016. [Online]. Available: http://journals.sagepub.com/doi/10.1177/1759313116649967

[4] Y. Perignon, "Assessing accuracy in the estimation of spectral content in wave energy resource on the french atlantic test site semrev," *Renewable Energy*, vol. 114, pp. 145–153, 2017.

[5] IEC, "IEC 62600-100 TS Ed.1: Marine energy Wave, tidal and other water current converters Part 100: Power performance assessment of electricity producing wave energy converters," International Electrotechnical Commission, Tech. Rep., 2012.

[6] H. Mouslim, A. Babarit, A. Clement, and B. Borgarino, "Development of the french wave energy test site sem-rev," in *Proceedings of the 8th European wave and tidal energy conference*, 2009, pp. 31–35.

[7] Y. Perignon and I. Le Crom, "Challenging best knowledge to real conditions on the semrev marine test site," in *Proceedings of the 11th European wave and tidal energy conference*, 2015.

[8] G. S. Payne, R. C. R. Pascal, and G. Vaillant, "On the concept of sloped motion for free-floating wave energy converters," *Proceedings of the Royal Society A*, vol. 417, no. 2182, 2015.

[9] R. C. R. Pascal and G. S. Payne, "Impact of motion limits on sloped wave energy converter optimization," *Proceedings of the Royal Society A*, vol. 472, no. 2187, 2016. [Online]. Available: http://rspa.royalsocietypublishing.org/content/472/2187/20150768

[10] Det Norske Veritas, "Environmental conditions and environmental loads," Tech. Rep. August, 2017.

[11] A. D. D. Andres, A. Macgillivray, R. Guanche, and H. Jeffrey, "Factors affecting LCOE of Ocean energy technologies: a study of technology and deployment attractiveness," in *5th International Conference on Ocean Energy*, Halifax, Canada, 2014, pp. 1–11.

[12] S. Astariz and G. Iglesias, "The economics of wave energy: A review," *Renewable and Sustainable Energy Reviews*, vol. 45, pp. 397–408, 2015.

[13] Y. Perignon and C. Maisondieu, "Assessing accuracy of hindcast spectral content in the estimation of wave energy resource," in *Proceedings of the 12th European wave and tidal energy conference*, 2017.

[14] S. Barrett, B. Holmes, and A. Lewis, "Monitoring of Seaway Variability on WEC Performance," in *Proceedings of the 2nd International Conference on Ocean Energy*, no. October, Brest, France, 2008, pp. 1–9.

[15] A. D. D. Andres, J. Maillet, J. Hals Todalshaug, P. Moller, and H. Jeffrey, "On the optimum sizing of a real WEC from a techno-economic perspective," in *Proceedings of the 34th International Conference on Ocean, Offshore and Arctic Engineering.* Busan, South Korea: American Society of Mechanical Engineers, 2016, p. 11.